

Abbreviations

%N	percentage nitrogen by mass
2-NDPA	2-Nitrodiphenylamine
a.u.	atomic units
B3LYP	Becke, 3-parameter, Lee-Yang-Parr hybrid functional
BCP	bonding critical point
CH₃CH₃	NC repeat unit with two methoxy capping groups
CH₃OH	NC repeat unit with methoxy capping group on ring 1, hydroxy group on ring 2
CCP	cage critical point
CP	critical point
DFT	density functional theory
DSC	differential scanning calorimetry
DOS	degree of substitution
DPA	diphenylamine
EM	energetic materials
ESP	electrostatic potential
G09	Gaussian 09 revision D.01
GM	genetically modified

GView	Gauss View 5.0.8
HF	Hartree Fock theory
IR	infra-red spectroscopy
MEP	minimum energy path
MM	molecular mechanics
MMFF94	Merck molecular force field 94
MW	molecular weight
NC	nitrocellulose
NCP	nuclear critical point
NG	nitroglycerine
NMR	nuclear magnetic resonance spectroscopy
OHCH₃	NC repeat unit with hydroxy capping group on ring 1, methoxy group on ring 2
PCM	polarisable continuum model
PES	potential energy surface
PETN	pentaerythritol tetranitrate
QM	quantum mechanics
QTAIM	quantum theory of atoms in molecules
RCP	ring critical point
SB59	1,4-bis(ethylamino)-9,10-anthraquinone dye
SEM	scanning electron microscopy
S_N2	bi-molecular nucleophilic substitution reaction
TG	thermogravimetric analysis

TS	transition state
UFF	universal force field
UV	ultraviolet
UV-Vis	ultraviolet-visible spectroscopy
ωB97X-D	ω B97X-D long-range corrected hybrid functional

Chapter 4

Post-Denitration Reactions

4.1 Introduction

Products of the preliminary denitration step of nitrocellulose (NC) can be evolved as gases or remain trapped in the polymer matrix. Reactive nitrous oxide radicals generated from homolysis of the O-N bond are likely to migrate within the bulk and attack other sites on the polysaccharide. Nitrous and nitric acids released directly from denitration, or via transformation of released NO_x species, contribute to the acidity of the overall system, lowering the pH and stimulating further hydrolysis processes [1].

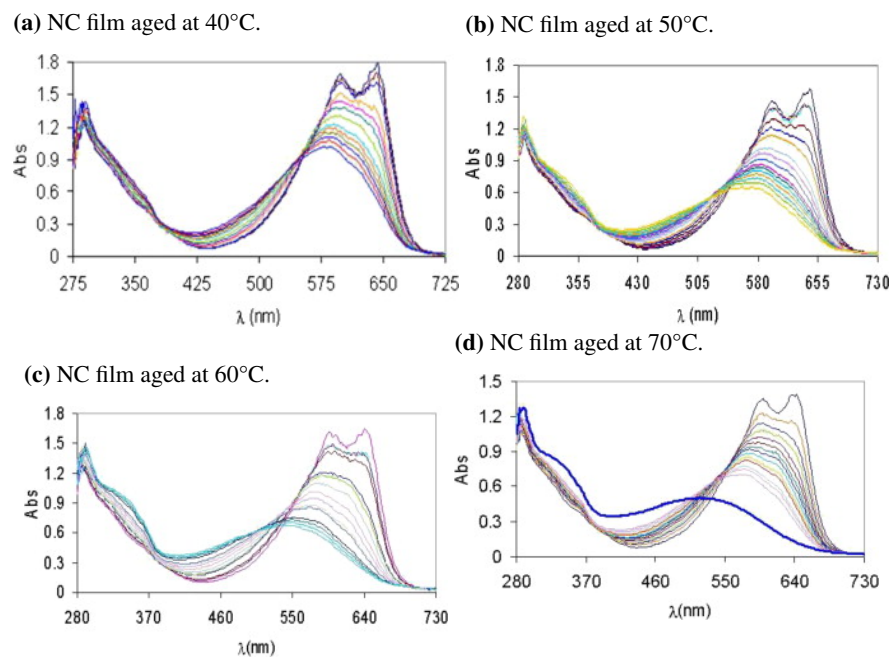
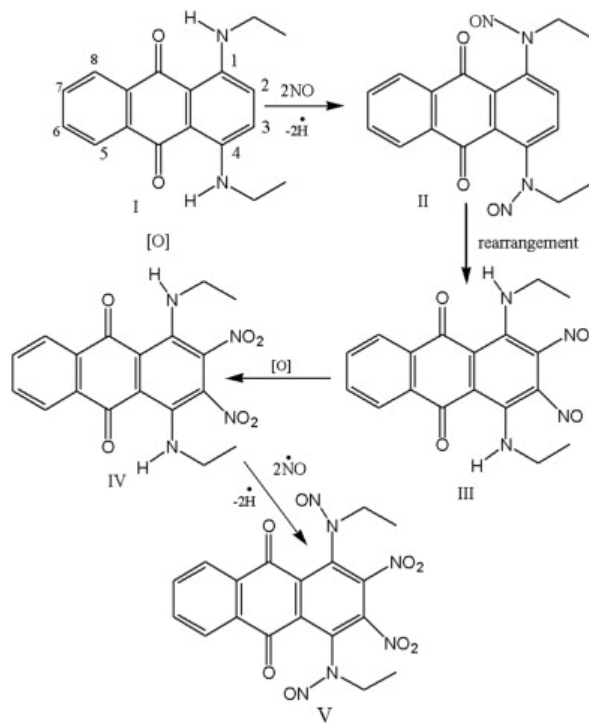


Figure 4.1: UV-Vis spectra of aged NC-based film, from the work of Moniruzzaman *et al.*[2]. The peaks at 600 nm and 650 nm are attributed to the $\pi - \pi^*$ transitions in the anthraquinone dye (1,4-bis(ethylamino)-9,10-anthraquinone dye (SB59)). Spectral lines with highest absorbance peaks in this region correspond to the sample prior to heat treatment. Peaks below 400 nm indicate the formation of SB59 derivatives due to secondary reactions.

When studying the ageing of NC using UV-Vis spectroscopy, Moniruzzaman *et al.* observed increasing concentrations of secondary reaction products following heat treatment over extended timescales[3, 2]. Samples exposed to higher ageing temperatures presented spectra dominated by consecutive products (figure 4.1). UV absorbances at 600 nm and 650 nm were characteristic of the SB59 dye used to indicate the presence of NO_x, released by the denitration of NC. The isosbestic point identified at 552 nm showed that as the concentration of SB59 decreased, the concentration of the [SB59 + NC] product increased. For sample aged at temperatures >40°C, the isosbestic point demonstrated a downwards shift. In the case of the 70°C treated run, the final measurement (indicated by the royal-blue line in bold, figure 4.1d) deviated from the isosbestic point entirely, and showed more than 81% consumption of the original dye concentration. The drift from the isosbestic point, in addition to the appearance of new absorbance peaks below 400 nm, alludes to the presence of new species in the reaction mixture not generated by the primary reaction of SB59 and NC. It is likely that these arise from the continued reaction of SB59 derivatives with NC degradation products, or further derivatives thereof, as suggested in scheme 4.1.

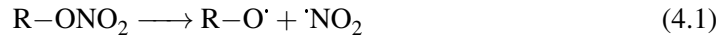


Scheme 4.1: Proposed pathway for the reaction of SB59 dye with ·NO released as a result of denitrination of NC [2].

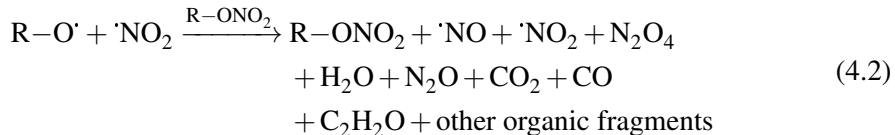
Following cleavage of the nitrate ester via homolytic fission, elimination of nitrous acid, or hydrolysis, the resulting residues are available for further reaction with the polymer

or other free molecules in the system. Chin *et al.* proposed schemes for the propagation of such reactions initiated by both the thermolysis and hydrolysis of nitrate esters [4]:

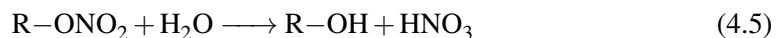
Thermolytic initiation



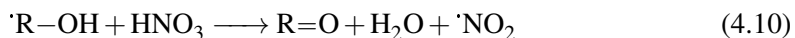
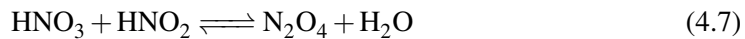
Propagation



Hydrolytic initiation

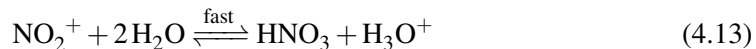
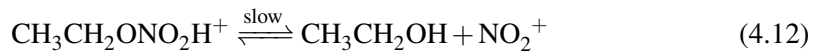


Propagation



Termination reactions were not emphasised in the schemes for either of these cases. The hydrolysis scheme was adapted from an earlier work by Camera *et al.* involving the nitrate ester decomposition and subsequent reactions of ethyl nitrate (where R = CH₃CH₂ for the scheme above) [5]. The original study included an expansion of the hydrolysis step (equation PhCH₂ONO₂,), where the involvement of NO₂⁺ is illustrated:

Hydrolysis scheme for ethyl nitrate

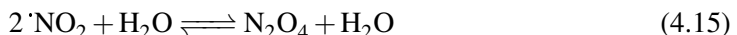


It was highlighted by Camera, that the oxidation of alcohol by nitric acid (equation 4.6) is slow and thus rate-limiting. The mechanism is likely to occur *via* a series of intermediate reactions of which the details are not known. Following the generation of nitrous acid, subsequent oxidations occur rapidly. According to Rigas *et al.*, alcohols are more susceptible to wet oxidation than esters [?]. A higher concentration of unsubstituted hydroxyl groups in the system, and therefore a fewer nitrate ester groups (or a lower degree of substitution (DOS) value), decreases overall stability.

Equations 4.7 - 4.10 describe a possible branched radical chain mechanism, fed by the nitrous and nitric acids produced during the hydrolysis and alcohol oxidation reactions during the initiation stage. By contrast, the propagation reactions in the branched radical chain mechanism for thermolysis are poorly characterised (equation 4.2), defined only by the observable products. This is likely due to their rapid and varied nature, rendering it difficult to follow spectroscopically.

Aellig *et al.* presented an alternative scheme for the decomposition of benzyl nitrate ($R = PhCH_2$), involving more interaction with the solvent [6]:

HNO₃ decomposition initiated



Propagation



Termination



Both the Camera/Chin and Aellig schemes above produce final end products observed in the decomposition of NC. In particular, Aellig's scheme accounts for the production of N₂O, which forms a significant part of the decomposition eluent [7]. Whilst the schemes do

not propose an exhaustive description of the full spectrum of reactions that take place in the NC matrix during its slow ageing, the early stage reactions of the key species responsible for decomposition are encapsulated.

It is widely agreed that first-stage decomposition follows a first-order process (or pseudo-first order, with respect to hydrolysis reactions). A number of studies observe catalytic rate of decay for the longer-term aging processes. Dauerman [8] observed that when NC was treated with NO_2 gas before heating, the time required for sample ignition halved. He suggested that the NO_2 adsorbed onto the surface acted as a catalysing agent.

Neutral and alkaline hydrolysis reactions follow a pseudo-first order process, however it has been suggested that the presence of acid facilitates a catalytic rate of degradation after an initial incubation period. Multiple studies have addressed the decomposition reactions of nitrate esters following the initial scission of the nitrate group [9, 5, 10, 11, 1]

In this section, secondary and extended reaction schemes for the low temperature ageing of NC are explored. Decomposition pathways defined by Chin, Camera and Aellig *et al.* are probed to determine the reactions responsible for the experimentally observed degradation products. The reactions found to be energetically feasible from the proposed routes will be scrutinised to determine whether an autocatalytic pathway can be formed from the thermodynamically validated reaction schemes.

4.2 Methodology

The reactions proposed by Chin, Camera and Aellig *et al.* were used to construct degradation routes for NC. The products of homolytic fission, elimination of HNO_2 and acid hydrolysis of NC were used as starting points. Schemes were constructed based on the propagation of the given reactions in a step-wise fashion; subsequent reactions were dependent on the products generated in prior steps, in addition to the assumed availability of other reactants in the system. An abundance of water and oxygen were assumed present in the system, attributed to air exposure or the wetted storage conditions of NC. Unsubstituted alcohol moieties (R-OH) were also presumed available, due to incomplete nitration during the synthesis of NC [12], or re-generation following denitration *via* hydrolysis. The schemes were modelled with both ethyl nitrate and the NC monomer. Free energies of reaction (ΔG) were used to determine the feasibility of a reaction.

4.2.1 Computational details

All geometry optimisations were performed in Gaussian 09 revision D.01 (G09), using the ω B97X-D long-range corrected hybrid functional (ω B97X-D) and Becke, 3-parameter, Lee-Yang-Parr hybrid functional (B3LYP) functionals. Optimisations were to the level of 6-31+G(2df,p) with tight convergence criteria (table ??). Chemical species were constructed using Gauss View 5.0.8 (GView) and for molecules of more than 3 atoms, the “Clean” function was used to re-order atoms to a preliminary reasonable geometry. Optimisations were performed in both vacuum and with polarisable continuum model (PCM) to introduce implicit solvent effects. Energies of optimised structures were checked against values listed on NIST Computational Chemistry Comparison and Benchmark Database [13] where available.

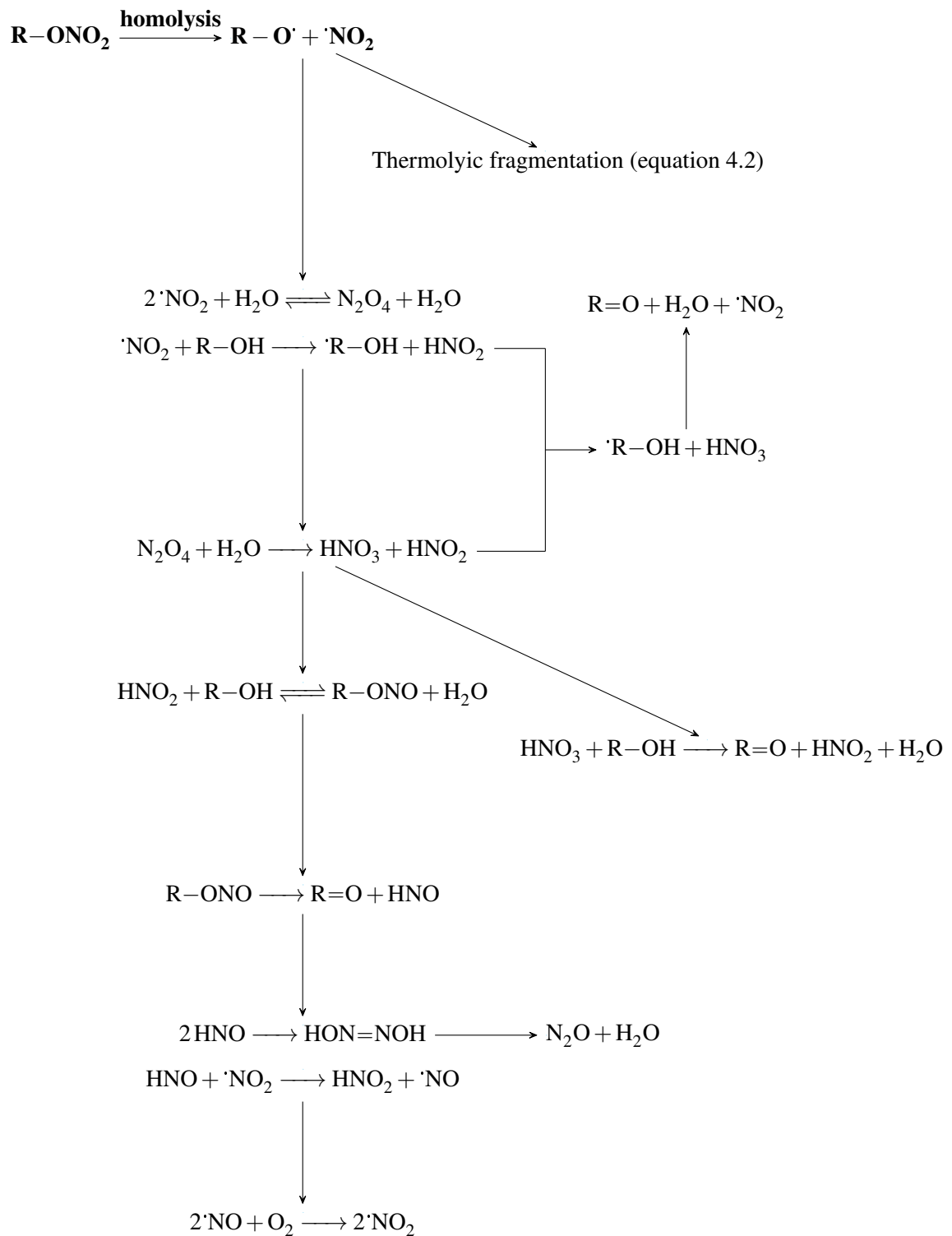
4.3 Results and Discussion

Simplified schemes for the ageing reactions of NC beginning from homolytic fission, elimination of HNO_2 or acid hydrolysis are illustrated in schemes 4.2 - 4.4. For the reactions starting from the products of homolytic fission, the propagation reactions are dominated by radical reactions. HNO_2 and $\cdot\text{NO}_2$ are consumed and regenerated, supporting the theory that these may be species contributing to the observed autocatalytic rate of decay, following a first-order rate induction period [14, 15, 16]. $\text{R}=\text{O}$ and N_2O are terminating species, though they may go on to participate in wider reactions outside the scope of the proposed reactions.

Still to mention:

- Describe the other two schemes
- Describe the energies in the table
- Discuss why some of the values may be positive.
- Include enthalpies of reaction, zero point energies, and any experimental proxies I can find for the reaction enthalpies too.
- ?

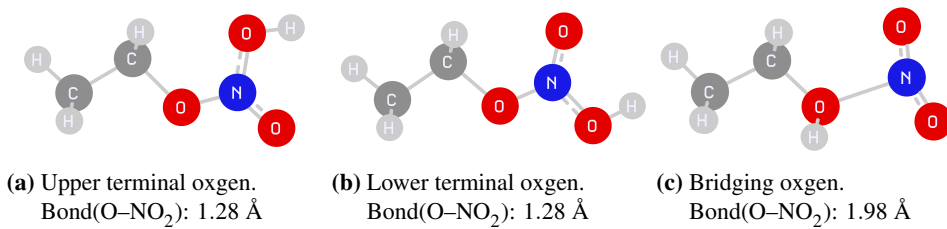
Due to the availability of oxygen sites on the ethyl nitrate molecule, the optimal site for protonation was determined for inclusion in the reaction scheme for the first stage of hydrolysis. Table 4.1 shows the protonation energies for the three different oxygen sites on ethyl nitrate. Despite the upper terminal oxygen possessing the most thermodynamically favourable energy of protonation, inspection of the reaction geometries shows that the



Scheme 4.2: Proposed degradation pathway starting from the homolysis products of a nitrate ester, derived from the schemes presented by Camera [5] and Aellig[6].

Table 4.1: Free energies of protonation for each oxygen site on ethyl nitrate.

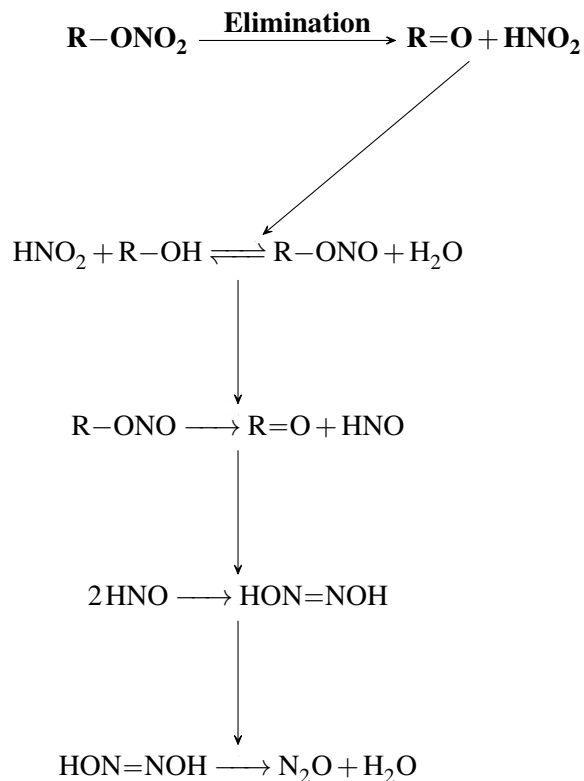
Protonated site		$\Delta G_r / \text{kcal mol}^{-1}$			
		$\omega\text{B97X-D}$	PCM	B3LYP	PCM
Terminal (upper)	$\text{CH}_3\text{CH}_3\text{ONO}_2\text{H}^+$	-12.2768	8.8219	-13.7825	5.6253
Terminal (lower)	$\text{CH}_3\text{CH}_3\text{ONO}_2\text{H}^+$	-9.4752	9.4595	-11.1321	5.6461
Bridging	$\text{CH}_3\text{CH}_3\text{O}(\text{H}^+)\text{NO}_2$	-9.3227	9.0581	-15.3096	6.6736

**Figure 4.2:** Optimised geometries of the possible protonation sites on ethyl nitrate.

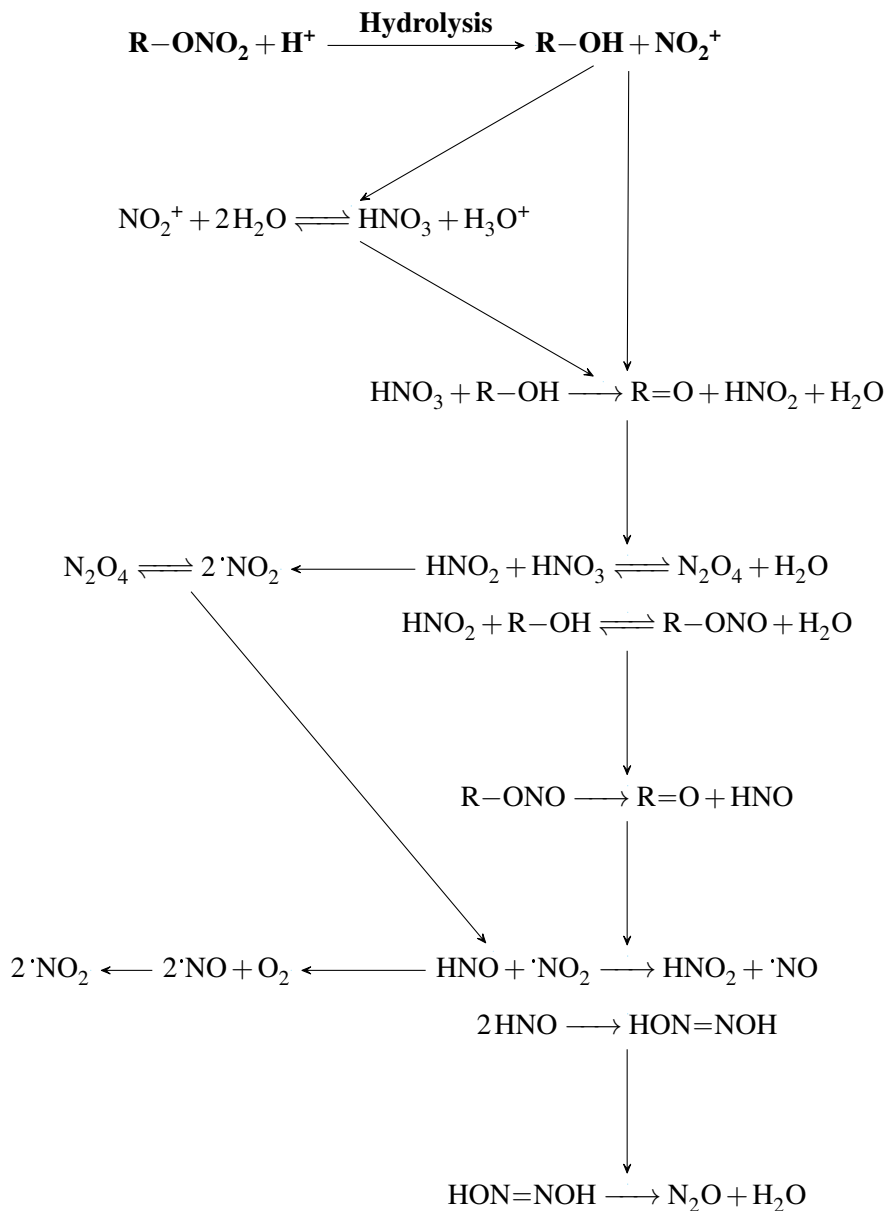
bridging structure most resembles that expected for the liberation of the NO_2^+ group at the next step. Though appearing less thermodynamically favourable when compared to protonation at the terminal upper oxygen site, the higher energy of reaction likely arises from the instability of the protonated complex. The elongation of the O-NO₂ bond allows to stabilisation of the proton at the bridging site, such that the departure of NO_2^+ is easily facilitated. Subsequent calculation involving the energy of the protonated ethyl nitrate will employ the values associated with the protonated bridging site.

For the decomposition of HNO_3 to NO_2 , $2\text{H}_2\text{O}$ and O_2 , Aellig prescribes the use of an amberlyst catalyst (amberlyst-15).

4.4 Summary



Scheme 4.3: Proposed degradation pathway starting from the elimination of HNO_2 from a nitrate ester, derived from the schemes presented by Camera [5] and Aellig[6].



Scheme 4.4: Proposed degradation pathway starting from the acid hydrolysis of a nitrate ester, derived from the schemes presented by Camera [5] and Aellig[6].

Table 4.2: Energies of nitrate ester decomposition reactions proposed by Camera [5], Chin [4] and Aellig [6]. R = CH₃CH₂ for ethyl nitrate, and R = (H₃CO)₂C₆H₉O₃ (bi-methoxy capped glucopyranose monomer unit).

Reaction	ΔG_r /kcal mol ⁻¹			
	ω B97X-D	PCM	B3LYP	PCM
NO ₂ ⁺ + 2H ₂ O \rightleftharpoons HNO ₃ + H ₃ O ⁺	-0.8965	-1.3388	1.7703	2.4646
2NO + O ₂ \longrightarrow 2NO ₂	-20.7705	-21.9731	-21.1604	-22.1590
2NO ₂ \rightleftharpoons N ₂ O ₄	-0.1222	-1.3104	0.5418	0.1556
HNO ₃ + HNO ₂ \rightleftharpoons N ₂ O ₄ + H ₂ O	-2.2516	-1.8541	-5.1314	-4.1801
N ₂ O ₄ \rightleftharpoons 2NO ₂	0.1235	1.4616	-0.5393	-0.1556
4HNO ₃ \rightleftharpoons 4NO ₂ + 2H ₂ O + O ₂	53.3503	58.3645	42.6094	46.9356
2NO ₂ + H ₂ O \rightleftharpoons N ₂ O ₄ + H ₂ O	-0.1222	-1.4616	0.5393	0.1556
N ₂ O ₄ + H ₂ O \longrightarrow HNO ₃ + HNO ₂	2.2516	1.8541	5.1314	4.1801
·NO ₂ + HNO \longrightarrow HNO ₂ + ·NO	-28.2164	-28.6682	-27.3269	-27.6255
2NO + O ₂ \longrightarrow 2NO ₂	-59.8947	-60.4724	-60.4687	-60.9960
2HNO \longrightarrow HON=NOH	-38.9693	-39.7158	-36.6276	-37.4081
HON=NOH \longrightarrow N ₂ O + H ₂ O	-48.0829	-48.1843	-50.5531	-50.7490
<hr/>				
Ethyl nitrate (R = CH ₃ CH ₂)				
R-OH + HNO ₃ \longrightarrow R=O + HNO ₂ + H ₂ O	-34.0622	-38.4275	-37.5940	-41.7703
R-OH + ·NO ₂ \longrightarrow ·R-OH + HNO ₂	16.3762	13.9230	15.8873	13.6994
·R-OH + HNO ₃ \longrightarrow R=O + H ₂ O + ·NO ₂	-50.4384	-52.3505	-53.4813	-55.4715
R-OH + HNO ₂ \rightleftharpoons R-ONO + H ₂ O	-3.2054	-3.2760	-2.6410	-2.9490
R-ONO \longrightarrow R=O + HNO	-1.4963	-5.8218	-4.3672	-8.5012
<hr/>				
NC monomer (R = (H ₃ CO) ₂ C ₆ H ₉ O ₃)				
R-ONO ₂ + H ₂ O \longrightarrow R-OH + HNO ₃	0.6754	5.6309	0.6124	-0.7012
R-OH + ·NO ₂ \longrightarrow ·R-OH + HNO ₂	14.7130	11.1516	13.0341	23.2098
·R-OH + HNO ₃ \longrightarrow R=O + H ₂ O + ·NO ₂	-51.4382	-49.4947	-54.7483	-56.3693
R-OH + HNO ₂ \rightleftharpoons R-ONO + H ₂ O	-4.4314	-7.3023	-4.3061	-0.1783
R-ONO \longrightarrow R=O + HNO	-2.9333	-1.7111	-6.8223	-11.2058

Bibliography

- [1] K. S. Hu, A. I. Darer, and M. J. Elrod. Thermodynamics and kinetics of the hydrolysis of atmospherically relevant organonitrates and organosulfates. *Atmospheric Chemistry and Physics*, 11(16):8307–8320, aug 2011.
- [2] Mohammed Moniruzzaman, John M. Bellerby, and Manfred A. Bohn. Activation energies for the decomposition of nitrate ester groups at the anhydroglucopyranose ring positions C2, C3 and C6 of nitrocellulose using the nitration of a dye as probe. *Polymer Degradation and Stability*, 102:49–58, apr 2014.
- [3] M. Moniruzzaman and J.M. Bellerby. Use of UV–visible spectroscopy to monitor nitrocellulose degradation in thin films. *Polymer Degradation and Stability*, 93(6):1067–1072, jun 2008.
- [4] Anton Chin, Daniel S. Ellison, Sara K. Poehlein, and Myong K. Ahn. Investigation of the Decomposition Mechanism and Thermal Stability of Nitrocellulose/Nitroglycerine Based Propellants by Electron Spin Resonance. *Propellants, Explosives, Pyrotechnics*, 32(2):117–126, apr 2007.
- [5] E. Camera, G. Modena, and B. Zotti. On the Behaviour of Nitrate Esters in Acid Solution. II. Hydrolysis and oxidation of nitroglycol and nitroglycerin. *Propellants, Explosives, Pyrotechnics*, 7(3):66–69, jun 1982.
- [6] Christof Aellig, Christophe Girard, and Ive Hermans. Aerobe Alkoholoxidation mithilfe von HNO₃. *Angewandte Chemie*, 123(51):12563–12568, dec 2011.
- [7] S. J. Buelow, D. Allen, G. K. Anderson, F. L. Archuleta, and J. H. Atencio. Destruction of Energetic Materials in Supercritical Water. Technical report, AIR FORCE RESEARCH LABORATORY, 2002.

- [8] L. Dauerman and Y. A. Tajima. Thermal decomposition and combustion of nitrocellulose. *AIAA Journal*, 6(8):1468–1473, aug 1968.
- [9] John W. Baker and D. M. Easty. Hydrolytic decomposition of esters of nitric acid. Part I. General experimental techniques. Alkaline hydrolysis and neutral solvolysis of methyl, ethyl, isopropyl, and tert.-butyl nitrates in aqueous alcohol. *Journal of the Chemical Society (Resumed)*, 1952(0):1193–1207, 1952.
- [10] E. Camera, G. Modena, and B. Zotti. On the behaviour of nitrate esters in acid solution. III. Oxidation of ethanol by nitric acid in sulphuric acid. *Propellants, Explosives, Pyrotechnics*, 8(3):70–73, jun 1983.
- [11] V. G. Matveev and G. M. Nazin. Stepwise Degradation of Polyfunctional Compounds. *Kinetics and Catalysis*, 44(6):735–739, nov 2003.
- [12] Frank E. Wolf. Alkaline Hydrolysis Conversion of Nitrocellulose Fines. Technical Report October, oct 1997.
- [13] Russell D. Johnson III. NIST Computational Chemistry Comparison and Benchmark Database NIST Standard Reference Database Number 101, 2018.
- [14] I. Rodger and J. D. McIrvine. The decomposition of spent PETN nitration acids. *The Canadian Journal of Chemical Engineering*, 41(2):87–90, apr 1963.
- [15] Torbjörn Lindblom. Reactions in stabilizer and between stabilizer and nitrocellulose in propellants. *Propellants, Explosives, Pyrotechnics*, 27(4):197–208, sep 2002.
- [16] Hermann N. Volltrauer and Arthur Fontijn. Low-temperature pyrolysis studies by chemiluminescence techniques real-time nitrocellulose and PBX 9404 decomposition. *Combustion and Flame*, 41:313–324, jan 1981.